



**HAL**  
open science

## A small-angle neutron scattering study of the ferrosmectic phase

Virginie Ponsinet, Pascale Fabre, Madeleine Veyssie, Loïc Auvray

► **To cite this version:**

Virginie Ponsinet, Pascale Fabre, Madeleine Veyssie, Loïc Auvray. A small-angle neutron scattering study of the ferrosmectic phase. *Journal de Physique II*, 1993, 3 (7), pp.1021-1039. 10.1051/jp2:1993179 . jpa-00247880

**HAL Id: jpa-00247880**

**<https://hal.science/jpa-00247880>**

Submitted on 4 Feb 2008

**HAL** is a multi-disciplinary open access archive for the deposit and dissemination of scientific research documents, whether they are published or not. The documents may come from teaching and research institutions in France or abroad, or from public or private research centers.

L'archive ouverte pluridisciplinaire **HAL**, est destinée au dépôt et à la diffusion de documents scientifiques de niveau recherche, publiés ou non, émanant des établissements d'enseignement et de recherche français ou étrangers, des laboratoires publics ou privés.

Classification

*Physics Abstracts*

82.70D — 61.30E — 61.12E

## A small-angle neutron scattering study of the ferrosmectic phase

Virginie Ponsinet <sup>(1)</sup>, Pascale Fabre <sup>(1)</sup>, Madeleine Veysie <sup>(1)</sup> and Loïc Auvray <sup>(2)</sup>

<sup>(1)</sup> Laboratoire de Physique de la Matière Condensée (\*), Collège de France, 11 place M. Berthelot, 75231 Paris Cedex 05, France

<sup>(2)</sup> Laboratoire Léon Brillouin (\*\*), Centre d'Etudes Nucléaires de Saclay, 91191 Gif sur Yvette Cedex, France

*(Received 26 October 1992, revised 18 March 1993, accepted 13 April 1993)*

**Résumé.** — Les phases ferrosmectiques sont des phases lamellaires gonflées non-conventionnelles qui contiennent, au sein des couches liquides, des particules colloïdales magnétiques. Ces systèmes, récemment mis au point, sont étudiés par diffusion des neutrons aux petits angles. Après de premières expériences effectuées sur la suspension magnétique tridimensionnelle pour déterminer les conditions de contraste appropriées à cette étude, nous analysons les paramètres de la phase lamellaire en fonction de son taux de gonflement et de la concentration en particules. Un des résultats les plus remarquables est l'évolution de l'intensité diffusée au pic de Bragg et aux très petits angles, qui est très différente de ce qu'on observe dans les phases lamellaires habituelles. Ces résultats permettent de conclure que l'interaction stabilisatrice effective n'est peut-être pas la répulsion d'Helfrich liée aux fluctuations des membranes, mais une interaction modifiée par la présence des particules.

**Abstract.** — The ferrosmectic phases are singular swollen lamellar phases whose peculiarity is to contain colloidal magnetic particles in their layers. A study of these newly invented systems by small angle neutron scattering is presented here. After a prior determination of the appropriate contrast conditions performed on the bulk magnetic suspension, we analyse the smectic features of the phases when varying the swelling ratio and the particle concentration. One of their most striking trends is the evolution of the Bragg and small angle scatterings, which are very different from conventional lamellar phases. We conclude from these results that the usual Helfrich repulsion related to the membrane fluctuations might be modified here by another stabilizing effect due to the presence of the particles.

### Introduction.

The ferrosmectic is a new lamellar system whose existence and stability have been established [1, 2] recently. It is constituted of lyotropic lamellar phase in which submicronic particles of

---

(\*) URA-CNRS 0792.

(\*\*) Laboratoire commun CEA-CNRS.

magnetic iron oxide are incorporated. The lamellar structure of the hybrid system has been checked under polarizing microscope where typical oily-streak defects [2, 3] are observed, as well as by preliminary X-ray scattering experiments. These systems, in addition to their optical anisotropy, exhibit a magnetic anisotropy [1, 4], as shown by the reorientation of the lamellae under a magnetic field.

These new materials are interesting from several points of view [5]. To our knowledge, the ferrosmelectics are the first example of compatibility between a spatially organized liquid and a solid colloid [6]; secondly, they may be considered as stackings of bidimensional magnetic fluids and lastly, they are smectic phases which exhibit a very low threshold field in magnetic instability ( $10^4$  times less than what is predicted in conventional smectics [7]).

For all these reasons, it is essential to acquire a precise knowledge of the structural features of the ferrosmelectics. To this purpose, the small-angle neutron scattering method is an appropriate tool insofar as the contrast variation technique allows different parts of the system to be seen independently. Moreover, the analysis of the spectra will provide valuable information on the nature of the stabilizing interactions in the system, which is indeed a crucial problem both in general and in this new hybrid material. This analysis allows us to compare the ferrosmelectic system with the case of conventional lamellar phases in which the stabilizing processes, intensively studied in the last few years, can be of two different types, the membranes being maintained apart either by an electrostatic or by a steric repulsion (Helfrich), depending on the nature of the constituents.

This article presents a comprehensive study, by a neutron scattering technique, of the structure of the ferrosmelectics and of its evolution when varying the relevant parameters.

In the first paragraph, we describe the physico-chemical features of the ferrosmelectic phase. In the second one, we describe the experimental conditions and specially the contrast condition which had to be previously determined. The third paragraph displays the experimental results on ferrosmelectics, which will be discussed and tentatively interpreted in the last paragraph.

## 1. Description of the ferrosmelectic phase.

**1.1 THE LYOTROPIC LAMELLAR PHASE.** — In order to achieve a convenient adaptability of the liquid crystal phase to the magnetic colloid, we choose a quaternary mixture composed of water, oil (cyclohexane) and two surfactants, namely sodium dodecyl sulfate (SDS) and pentanol. The phase diagram of this system presents a wide lamellar region [8]; in particular, the smectic phase is stable for a large range of oil content, which allows us to vary the periodicity of the lamellar phase: we can thus « swell » the phase from a few nanometers up to 50 nm. We call  $\Phi_s$  the swelling ratio, which will be one of our relevant parameters:

$$\Phi_s = \frac{\text{oil volume}}{\text{membrane volume}}$$

We define the *membrane* as the layer formed by the water and the surfactant molecules. We have set the water/surfactant ratio equal to 2.5 in weight, which corresponds to a membrane thickness of 5 nm [9]. The periodicity of the smectic phase will be called  $d$ .

**1.2 THE FERROFLUID.** — The ferrofluid, synthesized by Cabuil [10, 11], is a colloidal suspension of maghemite ( $\gamma\text{-Fe}_2\text{O}_3$ ) particles in cyclohexane, stabilized against aggregation by a shell of organo-phosphorated surfactant molecules. The maghemite is a ferromagnetic iron oxide, whose saturation magnetization  $M_s$  is equal to  $3.8 \times 10^5 \text{ A.m}^{-1}$ . The particles, of size about 10 nm, are magnetic monodomains and the suspension exhibits a superparamagnetic behaviour [12].

We will use  $\varphi$  to denote the volume fraction of particles in cyclohexane.

In section 2 the characteristics of the size distribution of the particles and the surfactant shell surrounding them are given from SANS experiments on the bulk ferrofluid.

**1.3 THE FERROSMECTIC PHASE.** — By combining the two previous systems, we build a new phase in which the solid particles are confined within the oil layer between two membranes. This is fulfilled by swelling the lyotropic phase with the ferrofluid instead of pure cyclohexane. Because of the size matching of the solid particles and lamellae on the one hand, and the chemical compatibility of the components on the other hand, the ferrosmectic phase does exist ; it is stable for a volume fraction in particles  $\varphi$  varying from 0.3 to 4 %, and for a smectic periodicity  $d$  in the range of 16 to 45 nm [13]. The swelling ratio  $\Phi_s$  is now defined by :

$$\Phi_s = \frac{\text{ferrofluid volume}}{\text{membrane volume}}$$

Figure 1 schematically represents the ferrosmectic phase. Note that this system is composed of two types of objects, the particles and the membranes, which are characterized by different coherent scattering lengths per unit volume. By selective deuteration of the solvent, one is able to vary the contrast in order to detect the scattering from either the particles alone or the membranes. The preliminary contrast variation experiments on the bulk ferrofluid presented in the next section are devoted to the determination of the zero contrast conditions for the particles.

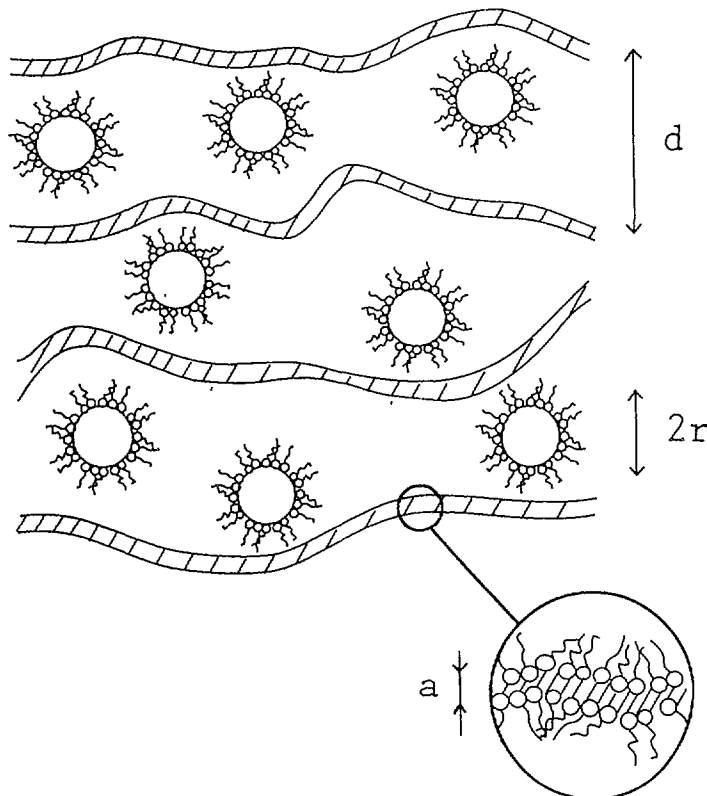


Fig. 1. — Structure of the ferrosmectic phase : membranes made of water and surfactant separate ferrofluid regions. Typical dimensions are  $d = 35$  nm,  $2r = 7$  nm,  $a = 5$  nm.

## 2. Experimental features.

**2.1 NEUTRON SCATTERING EQUIPMENT.** — The experiments were performed in the Laboratoire Léon Brillouin (Orphée reactor, Centre d'Etudes de Saclay, France) on the neutron line PAXY equipped with a two-dimensional detector. The non-polarized neutron beam has a wavelength  $\lambda = 7 \text{ \AA}$ . The distance between the sample and the counter is kept equal to 5 meters. In our experimental conditions, the wave vector ranges from  $q = 6 \times 10^{-3} \text{ \AA}^{-1}$  to  $q = 6 \times 10^{-2} \text{ \AA}^{-1}$ , with a resolution  $\Delta q = 3 \times 10^{-3} \text{ \AA}^{-1}$ . The samples are held in cells of thickness 1 mm. Absolute scale spectra are obtained by taking into account the incoherent scattering of water.

**2.2 DETERMINATION OF THE ZERO-CONTRAST CONDITION OF THE PARTICLES.** — In order to analyse the small-angle signal scattered by the membranes and be able to compare it to classical lamellar phases, we first have to determine the contrast condition under which the particles are matched by the cyclohexane.

Several contributions to the contrast between the particles and the solvent have to be taken into account : the nuclear contribution of the solid core, the nuclear scattering of the surfactant shell and the magnetic scattering (due to the interaction between the moment of the neutron and the magnetization of the matter) of the iron oxide. These three contributions are displayed in figure 2 which represents the profile of scattering density of a ferrofluid particle in a 50 %-deuterated solvent, as a function of the distance  $r$  to the center of the particle.

In order to determine the matching conditions, let us consider a sphere of radius  $R$  and effective density of scattering length  $n_{\text{eff}}$  (which contains both the nuclear and magnetic contribution of the iron oxide), coated by a shell of thickness  $t$  and density of scattering length  $n_s$ , and surrounded by a solvent of density of scattering length  $n_{\text{oil}}$ . The amplitude scattered by this object can be written :

$$a(q) = \int_{\text{sphere}} (n_{\text{eff}} - n_{\text{oil}}) e^{i\mathbf{q}\cdot\mathbf{r}} d\mathbf{r} + \int_{\text{shell}} (n_s - n_{\text{oil}}) e^{i\mathbf{q}\cdot\mathbf{r}} d\mathbf{r}. \quad (1)$$

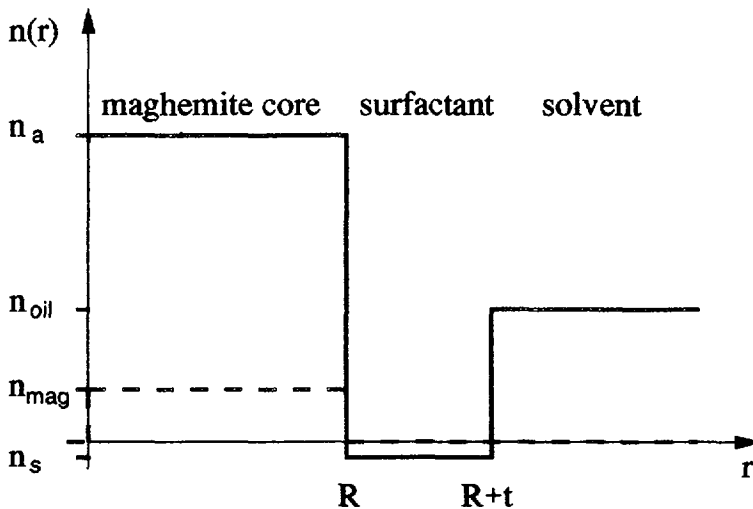


Fig. 2. — Profile of the density of scattering length of the ferrofluid particles in 50 %-deuterated solvent as a function of its radius. The dashed line corresponds to the magnetic scattering, whereas the continuous line represents the nuclear scattering. The values of the scattering length densities are  $n_n = 7.0 \times 10^{10} \text{ cm}^{-2}$ ,  $n_{\text{oil}} = 3.3 \times 10^{10} \text{ cm}^{-2}$ ,  $n_{\text{mag}} = 1.1 \times 10^{10} \text{ cm}^{-2}$ ,  $n_s = -0.4 \times 10^{10} \text{ cm}^{-2}$ .

In the limit where  $qR \ll 1$ , and if  $t$  is small compared to  $R$ , one can deduce from this expression the global zero contrast condition :

$$a(q \rightarrow 0) = \frac{4 \pi}{3} [(n_{\text{eff}} - n_{\text{oil}}^0) \langle R^3 \rangle + (n_s - n_{\text{oil}}^0) 3 t \langle R^2 \rangle] = 0 \quad (2)$$

where  $n_{\text{oil}}^0$  is the scattering density of the solvent which will match the particles.

$n_{\text{eff}}$  can also be expressed [14] by :

$$n_{\text{eff}} = \sqrt{n_n^2 + n_{\text{mag}}^2 \sin^2 \alpha} \quad \text{with} \quad n_{\text{mag}} = 1.913 \mu_n \frac{m}{2 \pi \hbar^2} 4 \pi M_s \quad (3)$$

where  $n_n$  is the nuclear contribution in the density of scattering length of the core,  $\alpha$  is the angle between the magnetic moment of the particle and the wave vector  $q$ ,  $M_s$  is the magnetization of the bulk maghemite,  $\mu_n$  is the nuclear magneton and  $m$  is the mass of the proton.

With  $m = 1.7 \times 10^{-24}$  g,  $\mu_n = 5.0 \times 10^{-24}$  erg/G,  $\hbar = 1.05 \times 10^{-27}$  erg.s,  $M_s = 380$  G, one finds that the magnetic contribution of the scattering density of the particle is  $n_{\text{mag}} = 1.1 \times 10^{10} \text{ cm}^{-2}$ , which is to be compared with the nuclear term  $n_n = 7.0 \times 10^{10} \text{ cm}^{-2}$

We can finally write the zero contrast condition :

$$n_{\text{oil}}^0 = \frac{\sqrt{n_n^2 + \frac{1}{3} n_{\text{mag}}^2 + n_s 3 t \frac{\langle R^2 \rangle}{\langle R^3 \rangle}}}{1 + 3 t \frac{\langle R^2 \rangle}{\langle R^3 \rangle}} \quad (4)$$

where the coefficient  $\frac{1}{3}$  comes from the averaging over the angles  $\alpha$ .

Whereas the pure nuclear scattering from iron oxide particles would be matched in a completely deuterated-solvent ( $n_n = 7.0 \times 10^{10} \text{ cm}^{-2}$ ,  $n_{\text{C}_6\text{D}_{12}} = 6.7 \times 10^{10} \text{ cm}^{-2}$ ), the matching condition will be obtained our case with a partially deuterated cyclohexane solvent.

The contrast variation experiment has been performed on ferrofluid samples of particle volume fraction  $\varphi = 1\%$  in which the deuterated/hydrogenated cyclohexane proportion is varied. Then, by plotting  $\sqrt{I_{q \rightarrow 0}}$  versus this ratio (Fig. 3), we have determined that the contrast is equal to zero for a 51%-deuterated ferrofluid. We have checked that this zero-contrast condition, which has been obtained at small wave-vectors  $q$ , remains valid on our whole range of  $q$ .

Besides, the study of the intensity scattered with the fully hydrogenated samples allows us to determine the two characteristics of the size distribution of the particles, which are the mean diameter and the standard deviation, since the contrast between the surfactant and the hydrogenated solvent is very low.

A log-normal type distribution for the diameter  $D$  of the particles is generally assumed [2] :

$$P(D) \propto \frac{1}{D} \exp\left(-\frac{1}{2 \sigma^2} \ln^2 \frac{D}{D_0}\right), \quad (5)$$

where  $\ln D_0$  is the average value of  $\ln D$  and  $\sigma$  is the standard deviation.

From the analysis of the neutron scattering spectra  $I(q)$ , one can obtain :

$$D_0 = 55.8 \text{ \AA} \quad \text{and} \quad \sigma = 0.47.$$

We will use this size distribution of the « naked » particles in the following.

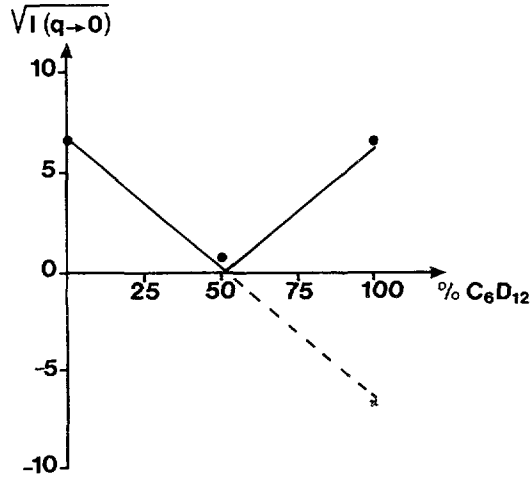


Fig. 3. — Plot of the square root of the intensity scattered, at small wavevector, by the bulk ferrofluid as a function of the fraction of deuterated solvent. The scattered intensity is zero for a 51 %-deuterated solvent (zero-contrast condition).

Since we now have experimental determinations of the zero-contrast solvent composition  $n_{oil}^0$  and the particle size distribution, we can obtain from equation (14) the value of the thickness  $t$  of the surfactant shell coating the particles. With  $n_{oil}^0 = 3.3 \times 10^{10} \text{ cm}^{-2}$ ,  $\frac{\langle R^3 \rangle}{\langle R^2 \rangle} = \frac{D_0}{2} e^{2.5 \sigma^2} = 48.6 \text{ \AA}$  [15] and  $n_s = -0.4 \times 10^{10} \text{ cm}^{-2}$ , one obtains  $t = 16.2 \text{ \AA}$ . This value corresponds to what can be expected for the size of our surfactant whose aliphatic tail contains about 30 carbon atoms and has a non-fully stretched configuration.

This preliminary study allows us to conclude that the particles are globally matched, including the magnetic scattering which is isotropic in the absence of a field, in a 51 %-deuterated solvent. All the experiments on ferrosmelectics presented here are carried out under this matching condition : all the features of the spectra are thus only due to the lamellae (cf. Appendix).

**2.3 FERROSMELECTIC SAMPLE PREPARATION.** — The experiments were performed on ferrosmelectic samples of different values of particle volume fraction  $\varphi$  ranging from 0.8 to 3.6 %, and for which we varied the swelling ratio  $\Phi_s$  between 2.2 and 5.0 (corresponding to periodicities between 20 and 40 nm), and on non-doped lamellar phase samples whose swelling ratio  $\Phi_s$  was varied between 2.0 and 5.2 (i.e. periodicities between 16 and 35 nm).

In these anisotropic phases, the orientation of the lamellar structure is essential. The samples are held in square capillaries with a cross-section  $1 \times 1 \text{ mm}$  and in this geometry, the doped or non-doped lamellae tend to orient perpendicular to the axis of the capillary. However, this spontaneous orientation is not satisfactory enough for our experiments.

In the ferrosmelectics, owing to the magnetic anisotropy [1] of the material, it is easy to enhance this orientation by the action of a weak rotating magnetic field parallel to the layer plane i.e. perpendicular to the capillary axis. All the ferrosmelectic spectra will be compared under the same conditions of orientation. Let us underline that the orientational effects are indeed very large, since the experiments have shown that the peak height is multiplied by a factor 50 when the orientation is achieved.

A difficulty arises when we want to compare the magnetic phases to the non-doped phases

which are insensitive to the magnetic field and for which it is difficult to monitor the quality of orientation. In order to have comparable information in this case, we have chosen to work with powder samples. This was achieved by quenching the phases from the isotropic high-temperature state. We check after this treatment that the neutron spectra are totally isotropic. In figure 4, are shown the spectra corresponding to an oriented and a powder sample of ferrosmectic.

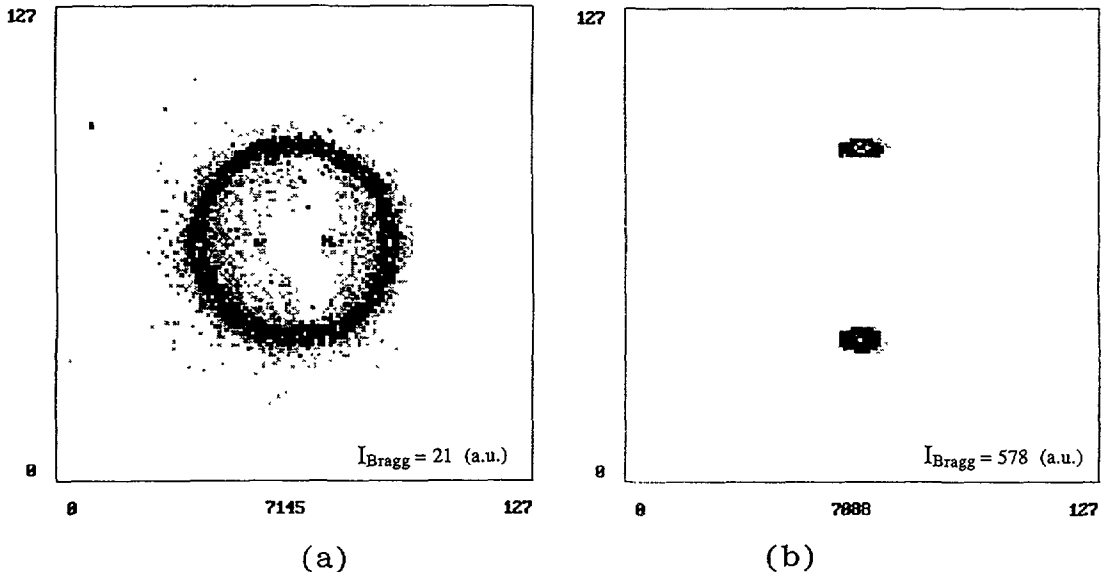


Fig. 4. — Two-dimensional spectra obtained on the PAXY line of the Laboratoire L. Brillouin (Orphée reactor, Centre d'Etudes de Saclay, France), on a ferrosmectic phase ( $\Phi_s = 2.9$ ,  $\varphi = 2.6\%$ ): a) powder sample quenched from isotropic state; b) oriented sample obtained by application of a rotating magnetic field.

### 3. Ferrosmectic phase : experimental results.

**3.1 MAIN FEATURES OF THE SPECTRA.** — Typical spectra obtained by small-angle scattering experiments performed on both conventional and doped powder samples are shown in figure 5. The meaningful features of the  $I(q)$  spectrum are the small-angle scattering signal (SAS) and the quasi-Bragg [16] peaks of first and possibly highest order which are the signature of the smectic structure. The position of the first Bragg peak  $q_0$  allows the determination of the smectic periodicity  $d$  along the relation  $q_0 = \frac{2\pi}{d}$ . We can already notice pronounced differences between a doped and a conventional phases having the same swelling ratio : for the conventional lamellar phase, the SAS and the Bragg intensities have the same order of magnitude and there is no second order peak ; for the ferrosmectic phase, the small-angle scattering diminishes, the Bragg-peak is strongly enhanced and a second-order shows up.

Let us now evaluate the influence of the form factor on this signal. For a unidimensionally periodic system, the intensity scattered in the direction of periodicity ( $q = q_z$ ) can be written

$$I(q) = (F(q))^2 S(q) \quad (6)$$



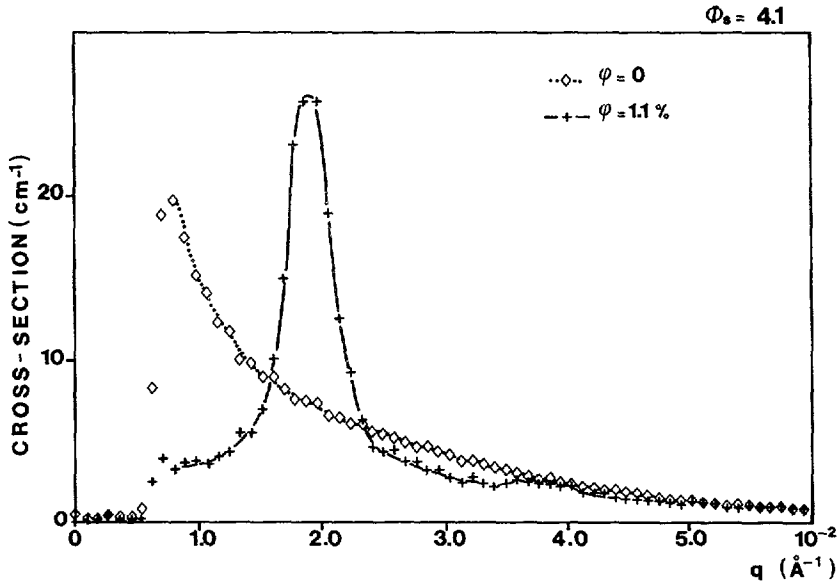


Fig. 5. — Comparison of the spectra of non-doped and doped lamellar phases at the same swelling ratio  $\Phi_s = 4.1$  for powder samples. The lines are guides for the eye.

where  $(F(q))^2$  is the form factor of the scattering object which is the square of the Fourier transform of the scattering density  $n(r)$  over one period, and  $S(q)$  is the structure factor which represents the inter-lamellae structure.

We are interested in the lamellar structure whose characteristics appear in the structure factor  $S(q)$ . We thus need to take into account the form factor  $(F(q))^2$  to analyse the experimental  $I(q)$ . The form factor can be calculated in a simple model in which the lamellar structure is assumed to be composed of perfectly flat and infinite lamellae and the scattering density profile of each lamella is approximated by a square function (cf. Fig. 6a) representing the respective densities of the solvent, the aliphatic tails of the surfactant molecules, their polar heads and the water. This form factor, although neglecting the membrane fluctuations, is relevant for the Bragg peak intensities. Figure 6b is a plot of  $(F(q_0))^2$ , the squared Fourier transform of the scattering length density  $n(x)$ , at the value  $q = q_0$ , as a function of  $q_0$ . Since the variation of  $(F(q_0))^2$  is small on the interesting  $q$ -range, the evolution of the peak intensities when varying the swelling ratio of the phase, described in the following, concerns indeed the smectic structure.

Notice that it is not possible to proceed to extract physical information from the lineshape analysis because the width of the quasi-Bragg peak is of the order of the resolution of the apparatus  $\Delta q = 3 \times 10^{-3} \text{ \AA}^{-1}$ , which is thus the limiting factor.

We will now discuss quantitatively the evolution of the main features of the spectra, namely the small angle scattering (SAS) and the diffraction peaks, as a function of two relevant parameters: the swelling ratio  $\Phi_s$  and the volume fraction in particles  $\varphi$ . We will particularly compare our results on ferrosmeectics with what we obtain with our non-doped lamellar phases, along with results concerning other comparable systems whose studies are described in references [17-20].

**3.2 EFFECT OF THE SWELLING RATIO  $\Phi_s$ .** — When we vary  $\Phi_s$ , keeping  $\varphi$  constant, both the position and the intensity of the Bragg peaks are modified (cf. Fig. 7). The shift of the Bragg

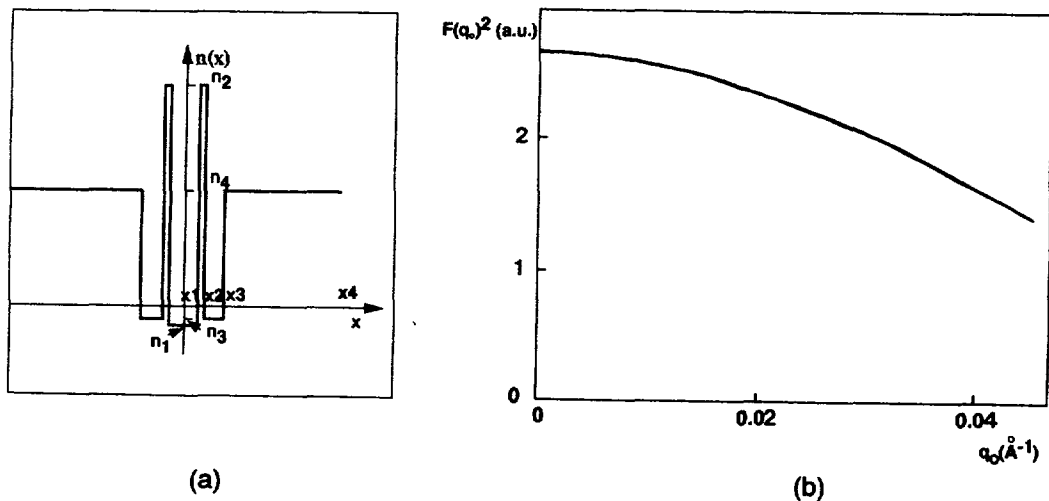


Fig. 6. — Form factor of ferrosmetic phases when matching the contrast of the particles : a) Profile of the density of scattering length  $n(x)$  of one lamella. The values of  $x_i$ , which indicates the respective sizes of the water layer, the polar heads of the surfactant molecules, their aliphatic tails and the periodicity of the phase, are  $x_1 = 14 \text{ \AA}$ ,  $x_2 = 20 \text{ \AA}$ ,  $x_3 = 30 \text{ \AA}$ ,  $x_4 = d/2$ . b) Form factor values  $(F(q_0))^2$  obtained by squared Fourier transform of  $n(x)$ , as a function of the Bragg peak position  $q_0$ .

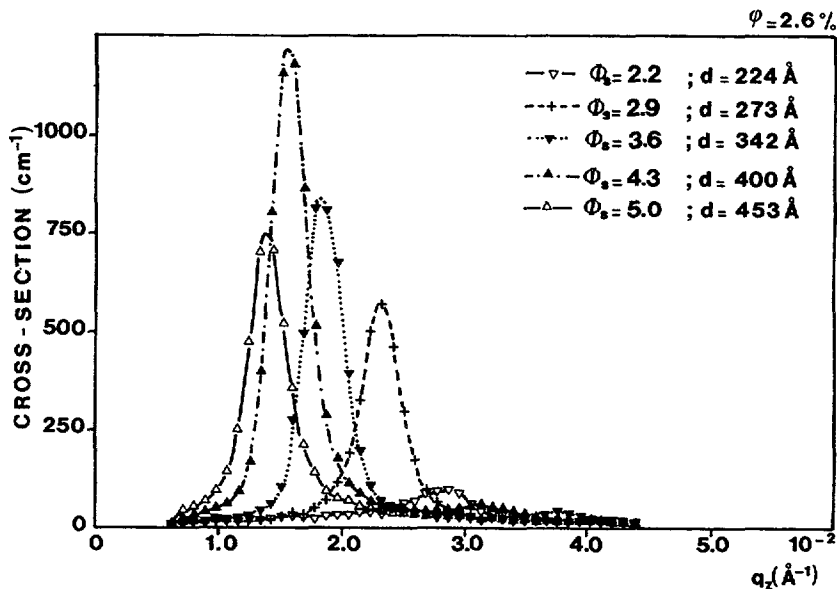


Fig. 7. — Evolution of the spectra when varying the swelling ratio at constant particle volume fraction :  $\varphi = 2.6 \%$ . The lines are guides for the eye.

peak is obviously related to an increase of the periodicity when we swell the lamellar phase. This increase of the periodicity  $d$  is larger than what would predict a simple swelling law for flat membranes :  $d = \delta (1 + \Phi_s)$ , with  $\delta$  the membrane thickness.

Considering now the intensity at the peak maximum, its evolution is less straightforward as

it first increases (in contrast to what is observed in conventional lamellar phases) and then, for the highest attainable swelling ratio ( $\Phi_s = 5.0$ ,  $\varphi = 2.6\%$ ), decreases. Moreover, a second-order peak appears clearly and its intensity follows the same evolution.

The SAS remains more or less constant, which is again different from conventional lamellar phases. Let us also notice that the SAS is weakly anisotropic.

**3.3 EFFECT OF THE VOLUME FRACTION OF PARTICLES  $\varphi$ .** — Let us first underline that the pronounced modifications of the spectra between undoped and doped phases, described in paragraph 3.1 appear as soon as a small amount of particles is added to the phases : the Bragg peak intensity sharply increases and we observe a significant fall of the SAS, even for very low concentrations ( $\varphi \approx 1\%$ ).

When varying the volume fraction  $\varphi$  of particles at constant swelling ratio  $\Phi_s$ , we observe that the Bragg peak is displaced. This implies that the periodicity varies whereas the phase contains the same quantity of oil (cf. Fig. 8a). More precisely, the periodicity is always larger than in the undoped phase of same swelling ratio, and the relative increment  $\frac{\Delta d}{d}$  first increases and then decreases for the highest particle concentrations. Note that this effect is much larger than the experimental uncertainty as the relative variation goes up to 15%.

Similarly, the intensity of the Bragg peak exhibits a non-monotonic variation (cf. Fig. 8b), with a change of slope for the same value of  $\varphi$  as for the periodicity. We also have to emphasize the existence of the second order harmonic, which is never observed in conventional oil swollen lamellar phases of the same range of periodicity. The intensity of this second-order peak follows the same variation law as the first one.

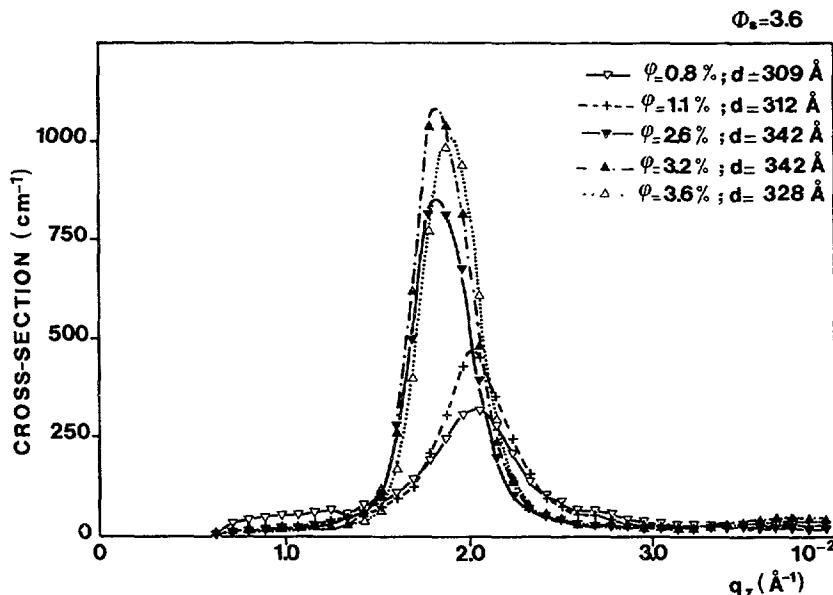


Fig. 8 a.

Fig. 8. — a) Evolution of the spectra when varying the particle volume fraction at constant swelling ratio  $\Phi_s = 3.6$ . The lines are guides for the eye. b) Plot of both the variation of the periodicity  $d$  of the doped lamellar structure (taken as the relative difference to the undoped corresponding phase) and the cross-section  $\sigma_B$  at the Bragg peak, normalized by a reference, as a function of the particle volume fraction  $\varphi$ , for two series of samples at  $\Phi_s = 2.9$  and  $\Phi_s = 3.6$ . The straight lines are guides for the eye.

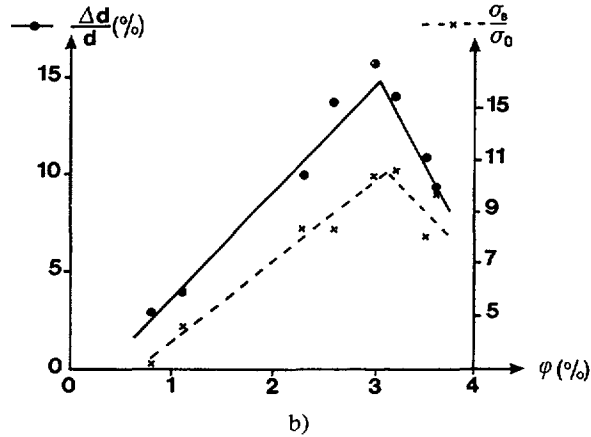


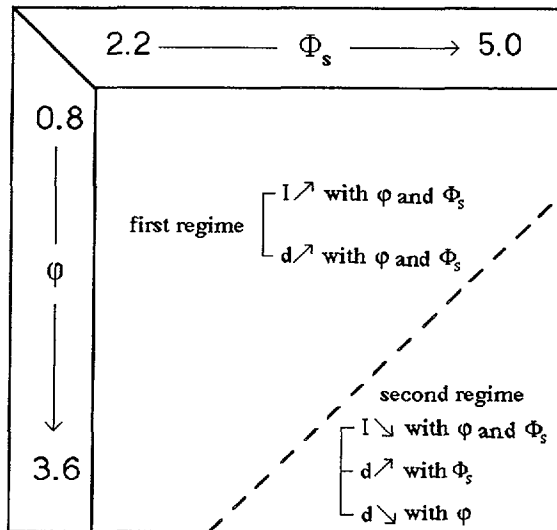
Fig. 8 (continued).

3.4 CONCLUSION. — Let us summarize the three main results from the experimental study :

- i) the spectra are radically different from what is found in conventional lamellar phases, concerning the evolution of the first peak intensity with the swelling ratio, the existence of a second-order Bragg peak, the weakness of the SAS. These differences clearly show a specific effect of the presence of the particles ;
- ii) the variation of the smectic periodicity with the swelling ratio is not trivial and depends on the particle volume fraction ;
- iii) the non-monotonic variations of the peak position and intensity imply the existence of two regimes depending on both  $\Phi_s$  and  $\phi$ .

The results are summarized in table I.

Table I. — Recapitulation of the evolution of the lamellar periodicity  $d$  and the intensity of the first Bragg peak  $I$  with the two parameters of the ferrosmectic phase :  $\Phi_s$  the swelling ratio and  $\phi$  the particle volume fraction. The dashed line is a mark of the border between the first and second regimes. For instance, for  $\Phi_s = 4.3$ , the change from first to second regime occurs for  $\phi = 2.6$  %.



#### 4. Discussion.

In the first three paragraphs of this chapter, we will discuss the results obtained in what we will call the first regime, i.e. for not too large values of  $\varphi$  and  $\Phi_s$ , by comparison with conventional lamellar phases, and propose a tentative interpretation. The fourth paragraph will be devoted to considerations about the existence of a second regime for larger values of  $\varphi$  and  $\Phi_s$ , a quantitative definition of the two regimes will be given there.

**4.1 INTRODUCTORY CONSIDERATIONS ON SMECTIC LYOTROPIC PHASES.** — The general trends of the spectra can be deduced from the expression of the free energy density of smectic-A lyotropic liquid crystal [21], which involves the thermal fluctuations of both the position of the lamellae  $u(\mathbf{r})$  and the membrane concentration  $\delta c$  :

$$F = \frac{1}{2} \left( B (\nabla \cdot u)^2 + K (\nabla_{\perp}^2 u)^2 + \frac{1}{\chi} \delta c^2 + 2 C \delta c \nabla \cdot u \right). \quad (7)$$

In this expression,  $z$  refers to the direction normal to the lamella stacking, and  $\perp$  to the directions within the plane ;  $B$  is the compressibility modulus at constant concentration ;  $K$  is the lamellar phase bending modulus, which can be related to the membrane bending modulus  $\kappa$  ;  $\chi$  is the osmotic compressibility of the membrane ; and  $C$  is a coupling constant between the surfactant concentration and the position fluctuations of the lamellae.

We also have to define the effective compressibility modulus  $\bar{B} = B - C^2 \chi$ . In the case where the membranes are incompressible,  $\bar{B}$  is the compressibility modulus at constant chemical potential and is derived from the interaction potential  $V(\ell)$  between membranes per unit surface area :

$$\bar{B} = d \left( \frac{\partial^2 V(\ell)}{\partial \ell^2} \right)_{\ell=d} \quad (8)$$

Because of the Landau-Peierls instability [22], the structure factor of the lamellar phases is not composed of Bragg peaks but of singularities existing at the Bragg positions ( $q_n = nq_0$  where  $n$  is the order of the peak and  $q_0$  is the position of the first order peak which is related to the smectic periodicity :  $q_0 = \frac{2\pi}{d}$ ), so that the intensity scattered in the directions normal and parallel to the layer plane can be written [16] :

$$I(0, q_z) \propto |q_z - q_n|^{-(2-n\eta)}, \quad q_n = nq_0 \quad (9)$$

$$I(q_{\perp}, q_n) \propto q_{\perp}^{-(4-2n^2\eta)} \quad (10)$$

The value of the characteristic exponent  $n^2 \eta$  for the peak of order  $n$  is related to the elastic constants of the smectic :

$$n^2 \eta = n^2 q_0^2 \frac{k_B T}{8 \pi \sqrt{K \bar{B}}}. \quad (11)$$

Expressions (9-11) show that the existence of a first order singularity requires that  $\eta$  should be smaller than 2 ; and the existence of a second order peak, that  $\eta$  should be smaller than 0.5 ; and that the values of the elastic constants  $K$  and  $\bar{B}$  intervene under these conditions.

As for the peak intensities, it has been predicted [23] that the height of the first-order Bragg

peak should scale as  $\frac{\lambda^{(1-\eta)}}{d^2}$  where the smectic penetration length [24]  $\lambda = \sqrt{\frac{K}{\bar{B}}}$  is a characteristic length related to the penetration of a surface distortion in a smectic sample.

Moreover, it is possible to proceed further if one has a microscopic model to describe the interactions stabilizing the system. Two types of long-range repulsive interactions are evoked to explain the stability of swollen phases, one of them being the electrostatic repulsion between charged layers and the other one the Helfrich entropic repulsion. As the initial swollen phase used for making ferrosmelectics belongs to the second category, we shall use its framework in a first attempt to interpret our results. Let us recall its main features. The stability of such a lamellar phase is the result of the balance between a van der Waals attraction which tends to the collapse of the membranes, and an entropic effect due to the confinement of the thermal fluctuations of the membranes. This entropic repulsion has been calculated by Helfrich [25] and may be written, in the limit of high swelling :

$$V(d) = \frac{3 \pi^2 (k_B T)^2}{128 \kappa d^2} \quad (12)$$

per unit membrane area, where  $\kappa$  is the membrane bending modulus defined before whose typical value lies between  $0.1 k_B T$  and  $1 k_B T$  [8, 19].

This has important consequences on the scattering spectra features. The expressions of  $K$ ,  $B$  and  $\bar{B}$  have been calculated [26], as well as the penetration length  $\lambda$  :

$$\lambda = \frac{8}{3 \pi} \frac{\kappa}{k_B T} d$$

and the value of  $\eta$ , which appears to be a constant independent of the system :  $\eta = \frac{4}{3}$ , in our range of periodicity [19].

Moreover, a pronounced and anisotropic SAS signal is observed and shown [18, 20] to be due to the magnitude of the membrane concentration fluctuations, which is increasing when the lamellar phase is swollen.

In summary, it has been shown that when  $d$  increases, in the case of Helfrich-type lamellar phases,

- i) the first-order Bragg peak intensity vanishes with a power-law  $d^{-7/3}$  ;
- ii) no Bragg peak except for the first order is expected ;
- iii) and the SAS increases like  $d$ .

**4.2 COMPARISON WITH FERROSMECTICS.** — It is clear that the model based on the Helfrich interaction is incompatible with our results, as far as the first regime is concerned : when we increase  $\Phi_s$  which implies that  $d$  increases,

- i) the first-order Bragg peak increases ;
- ii) the second-order appears ;
- iii) the SAS remains constant.

We are thus led to the conclusion that the Helfrich interaction is not dominant in our ferrosmelectic phases. In order to discuss our results, we will come back to the general features of smectic phases.

Let us recall that the existence of the second-order peak indicates that the characteristic exponent  $\eta$  is smaller than 0.5. This inequality is not consistent with the value predicted for Helfrich-type lamellar phases, and allows us to say that the product  $K\bar{B}$  is enhanced in the

doped phases : indeed, as compared to the corresponding non-doped Helfrich-type lamellar phase with the elastic constants  $K_H$ ,  $\bar{B}_H$  and  $\eta = \frac{4}{3}$ , we have (cf. Eq. (11)) :

$$K\bar{B} > \left(\frac{8}{3}\right)^2 K_H \bar{B}_H \approx 7 K_H \bar{B}_H. \quad (13)$$

Moreover, the difference of SAS signal between a doped and an undoped lamellar phase shows that in the first one the membrane concentration fluctuations have a much smaller magnitude ; this is linked to larger repulsive interactions between membranes resulting in an increase of  $\bar{B}$ , which is consistent with equation (13) (\*).

Moreover, the increase of the peak intensity with the periodicity  $d$  seems to indicate that  $\lambda$  should be quickly increasing with  $d$  :  $\lambda \propto d^\beta$  with  $\beta \geq \frac{2}{(1-\eta)} \geq 2$ .

**4.3 TENTATIVE INTERPRETATION.** — In order to understand the evolution of the smectic constants when incorporating the particles, one needs a microscopic model which differs from the Helfrich interaction for the stability of the smectic phase. The complexity of the phases makes this task uneasy but some tracks are given in the following.

First of all, we do not put forward any magnetic mechanism to explain the stability, as the dipolar interactions in such a dilute system are negligible [12] : the validity of this hypothesis is confirmed by a recent study of the stability and structure of the ferrosmectic phases compared to lamellar phases doped with non-magnetic particles which shows large similarities [13]. The specificity of the stability of ferrosmectics results thus from the presence of solid particles inside the layers and not from the own properties of their particles.

A first tentative interpretation is then to consider only the entropic effect due to the presence of the particles. In a very crude model where the particles are contained between two rigid and non-permeable walls, the inclusion of a translational-entropic term for the particles in the free energy of the system results in a repulsive effect on the walls, which can be expressed as the osmotic pressure of these particles.

Pincus suggested that such a perfect gas-type pressure [27]

$$\Pi_0 = \frac{3 k_B T}{4 \pi R^3} \varphi \quad (14)$$

(where  $R$  is the particle radius) can be of the same order of magnitude as the Helfrich-pressure deduced by the interaction potential per unit membrane area (cf. Eq. (12)) i.e.

$$\Pi_H = \frac{3 \pi^2 (k_B T)^2}{64 \kappa d^3} \quad (15)$$

and thus be linked to an enhancement of the compressibility  $\bar{B}$  of the phase. In fact, we will have  $\Pi_0 \approx \Pi_H$  if the system satisfies the condition :

$$\frac{16 \kappa}{\pi^3 k_B T} \left(\frac{d}{R}\right)^3 \varphi \approx 1. \quad (16)$$

(\*) This is also consistent with the weak anisotropy of the SAS observed in the ferrosmectic spectra, while a ratio of anisotropy of 100 has been predicted [18] in the Helfrich case. However, this argument is delicate to use as in conventional swollen lamellar phases, also, the theoretical ratio never seems to be experimentally observed : the current interpretation of this effect is that it is very sensitive to the quality of orientation of the sample.

With typical values of  $d = 30$  nm,  $R = 4$  nm and  $\varphi = 1$  %, we find  $\kappa$  of the order of  $0.5 k_B T$ , which is a reasonable value [8, 19]. Notice that  $\Pi_0$  is all the more dominant over  $\Pi_H$  as the value of  $\kappa$  is increased in the ferrosmeectics compared to non-doped lamellar phases.

The evaluation of this order of magnitude  $\Pi_0 \approx \Pi_H$  is interesting, but is based on a strong restriction which is the non-permeability of the membranes. Even if it has been experimentally proved by dynamic light scattering experiments that the diffusion coefficient of the particles perpendicular to the membranes is equal to zero [28], some permeation has to be considered for the system to achieve true thermodynamical equilibrium [29].

In any case, a detailed microscopic model for our complex system should take into account specific interactions between the particles and the membranes which may link the particle concentration, the membrane fluctuations and the periodicity of the phase, and lead to a non-uniform concentration profile of the particles in the layers [29].

Such a model should also account for the observed behaviour of the ferrosmeectic phase when varying the volume fraction of particles  $\varphi$  at constant swelling ratio  $\Phi_s$  and in particular the evolution of the smectic periodicity when we increase the particle concentration. Indeed, this effect is not easy to explain through simple qualitative arguments. The increase of the periodicity  $d$  at constant swelling ratio is linked to a diminution of either the membrane surface or the ratio between projected area and true membrane area.

The first effect could be due to a chemical mechanism corresponding to an exchange between the surfactants of the particles and the membranes. However, this hypothesis is hardly plausible since the sodium dodecyl sulfate is insoluble in cyclohexane while the observed variation of  $d$  would imply a large amount of exchanged molecules (of the order of the initial particle surfaction).

The diminution of the ratio between projected area and surface area might be due to an amplification of the membrane fluctuations, but this would mean a decrease of the elastic constant  $K$ , for which we do not have any experimental evidence, nor any microscopic model. On the contrary, the existence of an attractive interaction between the membranes and the particles, which would partly tend to be wrapped up in the molecular film and consume some membrane surface, would lead to the diminution of the effective area along with a stiffening of the membranes and thus an increase of  $K$ . Though it has to be kept in mind that a large part of the particles are free to move in the layers, as shown by light scattering experiments [29], this hypothesis due to Pincus is interesting since it would intervene in the stabilizing process of ferrosmeectics and have many other implications such as an essential role in the behaviour of ferrosmeectics under magnetic field implying a strong coupling between particles and membranes.

**4.4 CROSS-OVER BETWEEN THE TWO REGIMES.** — The interpretation presented before, which involves a new type of interactions stabilizing the ferrosmeectic lamellar system, was relative to what we called the first regime. In the second regime, the behaviour of the ferrosmeectics is modified although two « non-Helfrich »-type features (low SAS and existence of a second order peak) of the neutron scattering spectra remain valid (see Sect. 3).

An important fact to be recalled is that the first regime occurs for both low concentration  $\varphi$  in particles, and small swelling ratios : this can seem puzzling at first sight as it means that swelling the phase has the same effect as concentrating the particles. However, the relevant parameter to be considered might not simply be the mean distance between particles in the layers  $\xi_p$ , but rather its ratio to a typical length of the lamellar phase, such as the correlation length of the fluctuating membranes, which is of the order of  $d$ . Now, both processes of increasing  $\varphi$  or  $d$  lead to a decrease of the ratio  $\frac{\xi_p}{d}$ . Returning to the experimental results, one



then notes that the cross-over between the two regimes occurs for a ratio  $\frac{\xi_p}{d}$  which is close to unity : the effect of the particles on the lamellar phase is thus different whether they are closer or further to each other than the correlation length. We expect to get more information for discussing this interpretation from a small-angle scattering study on the order of the particles inside and across the layers, which is currently underway.

## 5. Conclusion.

The aim of the small-angle neutron scattering experiments presented here was to determine the structure of the new ferrosmectic phases quantitatively. By using conditions of contrast in which the scattered intensity is only due to the membranes, we analyse the evolution of the spectra with the relevant parameters of the system. This study allows us to point out some nonexpected effects : the periodicity does not depend only on the swelling ratio  $\Phi_s$ , but also on the particle volume fraction  $\varphi$ , there are two regimes of behaviour possibly linked to the interparticle correlations in the layers, and finally the main features of the spectra are strongly different from what is observed in non-doped lamellar phases.

This last point leads us, more precisely, to conclude that the dominant repulsive interaction balancing the van der Waals attraction in the ferrosmectic phases is not the Helfrich-type interaction which intervenes in classical lamellar phases, but is modified by the presence of the solid particles in a way that could be related to the particle entropy. Correlatively, the values of the compressibility modulus  $\bar{B}$  as well as the product  $K\bar{B}$ , with  $K$  the bending modulus, are enhanced by the presence of the particles.

These results are very promising for two main reasons. Firstly, the new type of stabilizing interactions found in the ferrosmelectics does not involve the magnetic character of the colloidal suspension ; we can thus imagine that the same kind of effects would be found with any solid suspension, as far as its physico-chemical compatibility is insured. Secondly, we can hope to swell lamellar systems for which, in the conventional situation, the Helfrich interaction is not strong enough, as far as we replace the pure solvent by a colloidal suspension.

We finally have to indicate that a study of the signal scattered by the particles, obtained when totally-hydrogenated cyclohexane is matching the membrane contrast, is underway and will give us complementary information about the interparticle structure and interactions.

## Acknowledgements.

This work is the result of a close cooperation with Valérie Cabuil and René Massart of the Laboratoire de Physico-chimie Inorganique, Université Pierre et Marie Curie, Paris and has benefited of an everyday collaboration with Catherine Quilliet and Raymond Ober. We have had numerous and fruitful discussions with F. Nallet, P. Pincus, J. Prost and M. Widom, whom we warmly thank.

## Appendix.

### Intensity scattered by a ferrosmectic.

We use a simplified model, where the lamellar phase is represented as a stacking of non-fluctuating parallel layers of water (thickness  $d_w$ ) and oil (thickness  $d_o$ ).

The coordinates of a point  $\mathbf{r}$  are  $\boldsymbol{\rho} = (x, y)$  parallel to the layers and  $z$  perpendicular to them. The scattering vector is also split up into a parallel component  $\mathbf{q}_{\parallel} = (q_x, q_y)$  and a perpendicular component  $\mathbf{q}_{\perp}$ . The local volume fractions of oil, water and particles are  $\Phi_o(r)$ ,  $\Phi_w(r)$  and  $\Phi_p(r)$  respectively. The respective scattering length densities are

$n_o$ ,  $n_w$  and  $n_p$ . For the sake of simplicity we do not take the contribution of the surfactant into account : neither the surfactant film of the smectic layers, nor the stabilizing surfactant sheet of the particles. This could be included in a further development.

We have the following relations of incompressibility : within a ferrofluid grain  $\Phi_p(\mathbf{r}) = 1$  ; within the oil layer  $\Phi_p(\mathbf{r}) + \Phi_o(\mathbf{r}) = 1$  ; on the whole  $\Phi_p(\mathbf{r}) + \Phi_o(\mathbf{r}) + \Phi_w(\mathbf{r}) = 1$ .

The scattering amplitude is then :

$$a(\mathbf{q}) = \int d^3\mathbf{r} e^{i\mathbf{q}\cdot\mathbf{r}} [n_p \Phi_p(\mathbf{r}) + n_o \Phi_o(\mathbf{r}) + n_w \Phi_w(\mathbf{r})].$$

At this point, we split up the local volume fractions into an average term and a fluctuating term :

$$\begin{aligned}\Phi_p(\mathbf{r}) &= \phi_p(z) + \delta\phi_p(z, \boldsymbol{\rho}) \\ \Phi_o(\mathbf{r}) &= \phi_o(z) + \delta\phi_o(z, \boldsymbol{\rho}) \\ \Phi_w(\mathbf{r}) &= \phi_w(z).\end{aligned}$$

Note that everywhere  $\delta\phi_p(z, \boldsymbol{\rho}) + \delta\phi_o(z, \boldsymbol{\rho}) = 0$ .

Correspondingly, the scattering amplitude breaks up into two terms :

$$a(q) = \bar{a}(q) + \tilde{a}(q)$$

with  $\bar{a}(q)$  the average scattering amplitude given by

$$\bar{a}(q) = \int d^3\mathbf{r} e^{i\mathbf{q}\cdot\mathbf{r}} [n_p \phi_p(z) + n_w \phi_w(z) + n_o \phi_o(z)]$$

and  $\tilde{a}(q)$  the fluctuating scattering amplitude written as

$$\begin{aligned}\tilde{a}(q) &= \int d^3\mathbf{r} e^{i\mathbf{q}\cdot\mathbf{r}} [n_p \delta\phi_p(z, \boldsymbol{\rho}) + n_o \delta\phi_o(z, \boldsymbol{\rho})] \\ &= (n_p - n_o) \int d^3\mathbf{r} e^{i\mathbf{q}\cdot\mathbf{r}} \delta\phi_p(z, \boldsymbol{\rho}).\end{aligned}$$

The expression of the average term can be further developed by taking into account the periodicity of the lamellar structure :

$$\bar{a}(q) = \left( \int d^2\boldsymbol{\rho} e^{i\mathbf{q}\cdot\boldsymbol{\rho}} \right) F(q_z) \sum_{n=-N/2}^{N/2} e^{iq_z n(d_o + d_w)}$$

with

$$F(q_z) = \int_{-d_o/2}^{d_o/2} dz e^{iq_z z} (n_p \phi_p(z) + n_o \phi_o(z)) + \int_{d_o/2}^{d_o/2 + d_w} dz e^{iq_z z} n_w.$$

The first term corresponds to the integration over the oil domains, the second to the integration over the water domains (where  $\phi_w(z) = 1$ ).  $F(q_z)$  is the form factor of the unit cell of the lamellar structure, which contains a contribution from the average concentration profile of the particles within the lamellae.

The scattering intensity is also the sum of two terms, an average term  $\bar{I}(q)$  and a fluctuation term  $\tilde{I}(q)$ . We write  $\bar{I}(q)$  as :

$$\bar{I}(q) = |F(q)|^2 S(q).$$

$S(q)$  is the classical structure factor of the smectic phase, which is non vanishing if the scattering vector  $q$  is normal to the lamellae.

Note that  $|F(q)|^2$  is a quadratic function of the Fourier Transform of the particle concentration profile within the lamella, which is obtainable in principle from a contrast variation experiment.

The fluctuation term  $\tilde{I}(q)$  arises simply from the intra and inter-lamellar correlations of the concentration fluctuations of the particle density in the oil layers. Its expression is classical and quite analogous to that of the bulk case :

$$\tilde{I}(q) = \langle |\tilde{a}(q)|^2 \rangle = (n_p - n_o)^2 \int d^3r e^{iq \cdot r} \int d^3r' e^{iq \cdot r'} \langle \delta \phi_p(r) \cdot \delta \phi_p(r') \rangle .$$

The simplest case is evidently obtained when the scattering length density of the particles matches that of the oil phase. There is no fluctuation term anymore, and the oil layers can be considered as homogeneous. The scattering intensity is thus directly comparable to what is obtained with the non-doped lamellar phase.

### References

- [1] FABRE P., CASAGRANDE C., VEYSSIE M., CABUIL V. and MASSART R., *Phys. Rev. Lett.* **64** (1990) 539.
- [2] FABRE P., OBER R. and VEYSSIE M., *J. Magn. Magn. Mater.* **85** (1990) 77.
- [3] FRIEDEL G., *Ann. Phys. France* **18** (1922) 273.
- [4] DABADIE J. C., FABRE P., VEYSSIE M., CABUIL V. and MASSART R., *J. Phys. Condens. Matter* **2** (1990) SA 291.
- [5] FABRE P., *Mat. Res. Soc. Symp. Proc.* **248** (1992) 55.
- [6] Concerning compatibility between colloidal suspensions and lyotropic nematics. see LIÉBERT L. and MARTINET A., *J. Phys. Lett. France* **40** (1979) L 363.
- [7] PARODI O., *Solid State Commun.* **11** (1972) 1503.
- [8] DI MEGLIO J. M., DVOLAITZKY M. and TAUPIN C., *J. Phys. Chem.* **89** (1985) 871 ; Physics of Complex and Supermolecular Fluids, S. A. Safran and N. Clark Eds. (New York, Wiley, 1987).
- [9] PONSINET V., FABRE P., VEYSSIE M. and AUVRAY L., to be published.
- [10] CABUIL V., thèse Université P. et M. Curie, Paris (1986).
- [11] MASSART R., *IEEE Trans. Magn.* **17** (1981) 1247.
- [12] ROSENSWEIG R. E., *Ferrohydrodynamics* (Cambridge University Press, Cambridge, 1985).
- [13] QUILLIET C., FABRE P. and CABUIL V., *J. Phys. Chem.* **97** (1993) 287.
- [14] SQUIRES G. L., Introduction to the theory of thermal neutron scattering (Cambridge University Press, Cambridge, 1978).
- [15] The moment of order  $n$  of a log-normal size distribution is expressed by
 
$$\langle R^n \rangle = \left( \frac{D_0}{2} \right)^n \exp \left( \frac{n^2}{2} \sigma^2 \right) .$$
- [16] CAILLÉ A., *C.R. Hebd. Acad. Sci. Paris* **B 274** (1972) 891.
- [17] BASSEREAU P., MARIGNAN J. and PORTE G., *J. Phys. France* **48** (1987) 673.
- [18] NALLET F., ROUX D. and MILNER S. T., *J. Phys. France* **51** (1990) 2333.
- [19] SAFINYA C. R., ROUX D., SMITH G. S., SINHA S. K., DIMON P., CLARK N. A. and BELLOCQ A. M., *Phys. Rev. Lett.* **57** (1986) 2718.
- [20] PORTE G., MARIGNAN J., BASSEREAU P. and MAY R., *Europhys. Lett.* **7** (1988) 713.
- [21] BROCHARD F. and DE GENNES P. G., *Pramāna Suppl.* **1** (1975) 1.

- [22] LANDAU L. D., *Phys. Z. Sowjetunion* **11** (1937) 26 ;  
PEIERLS R. E., *Helv. Phys. Acta Suppl.* **7** (1934) 81 ;  
ALS-NIELSEN J., LISTER J. D., BIRGENAU R. J., KAPLAN M., SAFINYA C., LINDEGAARD-ANDERSEN  
A. and MATHIESEN S., *Phys. Rev.* **B 22** (1980) 312.
- [23] GUNTHER L., IMRY Y. and LAJZEROWICZ J., *Phys. Rev.* **A 22** (1980) 1733.
- [24] DE GENNES P. G., *The physics of liquid crystals* (Clarendon Press, Oxford, 1974).
- [25] HELFRICH W., *Z. Naturforsch.* **33a** (1978) 305.
- [26] LUBENSKY T. C., PROST J. and RAMASWAMY S., *J. Phys. France* **51** (1990) 933.
- [27] PINCUS P., invited communication, 6th International Conference on Magnetic Fluids (Paris, July 1992).
- [28] FABRE P., QUILLIET C., VEYSSIÉ M., NALLET F., ROUX D., CABUIL V. and MASSART R.,  
*Europhys. Lett.* **20** (1992) 229.
- [29] NALLET F. and ROUX D., private communication.